

# Calculations of Higher Twist Distribution Functions in the MIT Bag Model

A. I. Signal

*Department of Physics, Massey University  
Palmerston North, New Zealand*

*and*

*Institute for Theoretical Physics, University of Adelaide SA 5005, Australia*

## Abstract

We calculate all twist-two, three and four parton distribution functions involving two quark correlations using the wavefunction of the MIT bag model. The distributions are evolved up to experimental scales and combined to give the various nucleon structure functions. Comparisons with recent experimental data on higher twist structure functions at moderate values of  $Q^2$  give good agreement with the calculated structure functions.

PACS numbers: 12.40.Aa, 13.60.Hb

Corresponding Author: Dr A I Signal Department of Physics Massey University, Private Bag 11-222 Palmerston North, New Zealand.

A.I.Signal@massey.ac.nz

Telephone: +64 6 350 4056 Fax: +64 6 354 0207

# 1 Introduction

Deep inelastic lepton - nucleon scattering (DIS) has been an important tool in particle physics for more than twenty-five years. Recent high precision measurements by groups such as the NMC, SMC and various SLAC groups [1, 2, 3, 4] are testing the limits of our theoretical knowledge of the structure of the nucleon. The SMC and the E143 groups [5, 6] have recently reported the first measurements of the transverse spin structure function  $G_2(x, Q^2)$ <sup>1</sup>, which has a twist-three component  $g_T$ . In the near future we can also expect the HERMES experiment to investigate the spin dependent structure functions in some detail. Also the development of polarized beams at RHIC will lead to measurements of the chiral-odd distributions  $h_{1,L}$ , which are twist-two and twist-three respectively [7].

Higher twist structure functions will also be important at the energies of CEBAF and the proposed ELFE accelerator because of the phenomenon of hadron-parton duality [8, 9], or ‘precocious scaling’ [10]. This predicts that at even moderate values of  $Q^2$ , higher twist contributions to observables, such as the nucleon form factor, will be non-negligible. Thus it is important to have some theoretical understanding on the expected sizes and shapes of the higher twist structure functions.

In a recent paper, Ji [11] defined the 14 possible nucleon structure functions in the standard model, and calculated each structure function in terms of all the possible parton distribution functions up to the level of twist-four (ignoring loop effects from QCD radiative corrections). The parton distribution (or correlation) functions are defined in terms of Fourier transforms of matrix elements of non-local quark and gauge fields separated

---

<sup>1</sup>Throughout this work I use capital letters  $F$ ,  $G$  to denote the structure functions measured in experiment and lower case letters  $f$ ,  $g$ ,  $h$  to denote the various parton distributions.

along the light-cone [7, 11, 12]. At present these matrix elements cannot be calculated in QCD, however calculations of twist-two matrix elements using the wavefunction of the MIT bag model have been performed [13, 14], and these describe current data relatively well. In this paper these calculations are extended to all the parton distribution functions of twist-three and four containing only two quark fields.

## 2 Parton Distribution Functions

Following Ji [11], let us consider a nucleon of mass  $M$  with momentum  $P^\mu$  and polarisation vector  $S^\mu$ . If we choose the nucleon to be moving along the  $z$ -axis with momentum  $P$  we have

$$P^\mu = (\sqrt{M^2 + P^2}, 0, 0, P). \quad (1)$$

We introduce two orthogonal, light-like vectors  $p$  and  $n$

$$\begin{aligned} p^\mu &= \frac{1}{2}(\sqrt{M^2 + P^2} + P)(1, 0, 0, 1), \\ n^\mu &= \frac{1}{M^2}(\sqrt{M^2 + P^2} - P)(1, 0, 0, -1), \end{aligned} \quad (2)$$

satisfying  $P^\mu = p^\mu + M^2 n^\mu / 2$ . We also decompose the polarisation vector,  $S = S_\parallel + M S_\perp$ , where

$$S_\parallel^\mu = p^\mu - \frac{M^2}{2} n^\mu, \quad S_\perp^\mu = (0, 1, 0, 0). \quad (3)$$

A parton distribution with  $k$  light-cone momentum fractions  $M(x_1, \dots, x_k)$  is defined via the matrix element

$$\int \prod_{i=1}^k \frac{d\lambda_i}{2\pi} \exp(i\lambda_i x_i) \langle PS | \hat{Q}(\lambda_1 n, \dots, \lambda_k n) | PS \rangle = M(x_1, \dots, x_k) \hat{T}(p, n, S_\perp) \quad (4)$$

where  $\hat{Q}$  is a product of  $k$  quark and gluon fields, and  $\hat{T}$  is a Lorentz tensor.

If the mass dimension of the parton distribution  $M(x_i)$  is  $d_M$  and that of  $\hat{T}$  is  $d_T$ , then at large  $Q^2$  the matrix element will behave as  $\Lambda^{d_M} Q^{d_T}$ , where  $\Lambda$  is a soft QCD mass scale related to non-perturbative physics. A distribution with mass dimension  $d_M$  is called a twist- $(d_M + 2)$  distribution. As the dimension of a physical observable is fixed, the higher  $d_M$  becomes, the higher the inverse power of hard momenta must become in the observable. Thus a twist- $n$  parton distribution can only contribute to physical observables of twist- $n$  or higher, which behave as  $Q^{2-(n+a)}$ , where  $a \geq 0$ , in the  $Q^2 \rightarrow \infty$  limit. In the following we will often rescale a parton distribution by factors of  $(M/\Lambda)$  to make it dimensionless, but the twist will be unchanged.

For scattering processes involving two quark fields we can define a quark density matrix

$$M_{\alpha\beta}(x) = \int \frac{d\lambda}{2\pi} e^{i\lambda x} \langle PS | \bar{\psi}_\beta(0) \psi_\alpha(\lambda n) | PS \rangle. \quad (5)$$

From this it is possible to systematically generate the possible distributions at a given twist. The twist-2 part of the density matrix can be written

$$M(x)|_{\text{twist-2}} = \frac{1}{2} \not{x} f_1(x) + \frac{1}{2} \gamma_5 \not{x} (S_\parallel \cdot n) g_1(x) + \frac{1}{2} \gamma_5 \not{x}_\perp \not{S}_\perp h_1(x) \quad (6)$$

where the three quark distribution functions  $f_1$ ,  $g_1$  and  $h_1$  are defined

$$\begin{aligned} f_1(x) &= \frac{1}{2} \int \frac{d\lambda}{2\pi} e^{i\lambda x} \langle P | \bar{\psi}(0) \not{x} \psi(\lambda n) | P \rangle, \\ g_1(x) &= \frac{1}{2} \int \frac{d\lambda}{2\pi} e^{i\lambda x} \langle PS_\parallel | \bar{\psi}(0) \not{x} \gamma_5 \psi(\lambda n) | PS_\parallel \rangle, \\ h_1(x) &= \frac{1}{2} \int \frac{d\lambda}{2\pi} e^{i\lambda x} \langle PS_\perp | \bar{\psi}(0) \not{x} \gamma_5 \not{S}_\perp \psi(\lambda n) | PS_\perp \rangle. \end{aligned} \quad (7)$$

These represent the unpolarized quark density, the quark helicity density and the quark transversity density [7] respectively. The light-cone gauge,  $A^+ = 0$ , has been chosen, so

that the distributions are manifestly gauge invariant.

Similarly at the twist-3 level, the appropriate portion of the quark density matrix can be written

$$M(x)|_{\text{twist-3}} = \frac{\Lambda}{2} [e(x) + \frac{1}{2}(S_{\parallel} \cdot n)(\not{\epsilon} \not{\epsilon} - \not{\epsilon} \not{\epsilon})\gamma_5 h_L(x) + \gamma_5 \not{\epsilon}_{\perp} g_T(x)] \quad (8)$$

where  $\Lambda$  is a soft mass scale in QCD. The three twist-3 distribution functions are given by

$$\begin{aligned} e(x) &= \frac{1}{2\Lambda} \int \frac{d\lambda}{2\pi} e^{i\lambda x} \langle P | \bar{\psi}(0) \psi(\lambda n) | P \rangle, \\ h_L(x) &= \frac{1}{2\Lambda} \int \frac{d\lambda}{2\pi} e^{i\lambda x} \langle PS_{\parallel} | \bar{\psi}(0) \frac{1}{2}(\not{\epsilon} \not{\epsilon} - \not{\epsilon} \not{\epsilon})\gamma_5 \psi(\lambda n) | PS_{\parallel} \rangle, \\ g_T(x) &= \frac{1}{2\Lambda} \int \frac{d\lambda}{2\pi} e^{i\lambda x} \langle PS_{\perp} | \bar{\psi}(0) \gamma_5 \not{\epsilon}_{\perp} \psi(\lambda n) | PS_{\perp} \rangle. \end{aligned} \quad (9)$$

At twist-4 we have

$$M(x)|_{\text{twist-4}} = \frac{\Lambda^2}{4} [\not{\epsilon} f_4(x) + \not{\epsilon} \gamma_5 (S_{\parallel} \cdot n) g_3(x) + \not{\epsilon} \gamma_5 \not{\epsilon}_{\perp} h_3(x)] \quad (10)$$

with the twist-4 distributions

$$\begin{aligned} f_4(x) &= \frac{1}{2\Lambda^2} \int \frac{d\lambda}{2\pi} e^{i\lambda x} \langle P | \bar{\psi}(0) \not{\epsilon} \psi(\lambda n) | P \rangle, \\ g_3(x) &= \frac{1}{2\Lambda^2} \int \frac{d\lambda}{2\pi} e^{i\lambda x} \langle PS_{\parallel} | \bar{\psi}(0) \gamma_5 \not{\epsilon} \psi(\lambda n) | PS_{\parallel} \rangle, \\ h_3(x) &= \frac{1}{2\Lambda^2} \int \frac{d\lambda}{2\pi} e^{i\lambda x} \langle PS_{\perp} | \bar{\psi}(0) \gamma_5 \not{\epsilon}_{\perp} \psi(\lambda n) | PS_{\perp} \rangle. \end{aligned} \quad (11)$$

The quark field  $\psi$  can be decomposed into ‘good’ and ‘bad’ components,  $\psi_+$  and  $\psi_-$  respectively

$$\psi_{\pm} = P^{\pm} \psi, P^{\pm} + \frac{1}{2} \gamma^{\mp} \gamma^{\pm}, \gamma^{\pm} = \frac{1}{\sqrt{2}} (\gamma^0 \pm \gamma^3). \quad (12)$$

By inspection it can be seen that the twist-2 quark distributions involve only the ‘good’ component  $\psi_+$ , whereas the twist-3 distributions involve mixing one ‘good’ and one ‘bad’ component, and the twist-4 distributions involve only the ‘bad’ components.

The QCD equations of motion [15]

$$i \frac{d}{d\lambda} \psi_-(\lambda n) = \frac{1}{2} \not{n} (-i \not{D}_\perp + m_q) \psi_+(\lambda n), \quad (13)$$

$$-i \frac{d}{d\lambda} \bar{\psi}_-(\lambda n) = \frac{1}{2} \bar{\psi}_+(\lambda n) (-i \not{D}_\perp + m_q) \not{n}, \quad (14)$$

make it possible to eliminate the ‘bad’ components from the twist-three and four distributions, at the cost of introducing gluon fields into the matrix elements. Because the model wavefunctions do not include gluon fields, we will not do this here. Also note that at twist-three and twist-four there exist distributions involving the gluon field with two or three light-cone momentum fractions, such as [11, 12]

$$E(x, y) = -\frac{1}{4\Lambda} \int \frac{d\lambda}{2\pi} \frac{d\mu}{2\pi} e^{i\lambda x} e^{i\mu(y-x)} \langle P | \bar{\psi}(0) i \not{D}_\perp(\mu n) \not{n} \psi(\lambda n) | P \rangle, \quad (15)$$

and

$$B_1(x, y, z) = \frac{1}{2\Lambda^2} \int \frac{d\lambda}{2\pi} \frac{d\mu}{2\pi} \frac{d\nu}{2\pi} e^{i\lambda x} e^{i\mu(y-x)} e^{i\nu(z-y)} \langle P | \bar{\psi}(0) \not{n} i \not{D}_\perp(\nu n) i \not{D}_\perp(\mu n) \psi(\lambda n) | P \rangle, \quad (16)$$

which can be related to  $e(x)$  and  $f_4(x)$  by integrating over  $y$  or  $y$  and  $z$  respectively. However, as the MIT bag wavefunction has no explicit gluon field, these distributions will be zero in the model. Also the distributions with only one light-cone momentum fraction are of the most interest for DIS and Drell-Yan processes.

Finally there exist distributions at the twist-four level involving four quark operators eg

$$U_1^s(x, y, z) = \frac{1}{4\Lambda^2} \int \frac{d\lambda}{2\pi} \frac{d\mu}{2\pi} \frac{d\nu}{2\pi} e^{i\lambda x} e^{i\mu(y-x)} e^{i\nu(z-y)} \langle P | \bar{\psi}(0) \not{n} \psi(\nu n) \bar{\psi}(\mu n) \psi(\lambda n) | P \rangle, \quad (17)$$

which is a four quark light-cone correlation function. Calculating this distribution by the method below would require the evaluation of the overlap integral between the four quark

fields over the bag volume, which is expected to much smaller than the two quark overlap integral required for the two quark correlation functions. Hence these will not be considered further in this work.

### 3 Calculation of Quark Distributions

At present no QCD wavefunction for the nucleon can be calculated. So in order to make useful calculations of the quark distributions at any twist it is necessary to use the wavefunction from some phenomenological model of the nucleon. The MIT bag model [16] is used here as it incorporates relativistic, light quarks, and also models confinement. It also has the further advantage that the wavefunction is simple and analytic. Other models could also be chosen [17].

The major problem in calculating the relevant matrix elements for the quark distributions is ensuring that momentum conservation is obeyed throughout the calculation, hence ensuring that the calculated distributions have the correct support, i.e. they vanish for light-cone momentum fraction  $x$  outside the interval  $[0, 1]$  [18]. To guarantee momentum conservation, a complete set of intermediate states,  $\sum_m |m\rangle\langle m|$ , can be inserted into the matrix elements of the quark distributions (eqns. (7, 9, 11)). Using translational invariance of the matrix element, all the  $n$  dependence can be moved into the argument of the exponential function. Then integrating over  $\lambda$  gives a momentum conserving delta function. The twist-two quark distributions then become

$$\begin{aligned} f_1(x) &= \frac{1}{\sqrt{2}} \sum_m \delta(p^+(1-x) - p_m^+) |\langle m | \psi_+(0) | P \rangle|^2, \\ g_1(x) &= \frac{1}{\sqrt{2}} \sum_m \delta(p^+(1-x) - p_m^+) [|\langle m | \hat{R} \psi_+(0) | PS_{\parallel} \rangle|^2 - |\langle m | \hat{L} \psi_+(0) | PS_{\parallel} \rangle|^2], \end{aligned}$$

$$h_1(x) = \frac{1}{\sqrt{2}} \sum_m \delta(p^+(1-x) - p_m^+) [|\langle m | \hat{Q}_+ \psi_+(0) | PS_\perp \rangle|^2 - |\langle m | \hat{Q}_- \psi_+(0) | PS_\perp \rangle|^2], \quad (18)$$

where  $\hat{R}(\hat{L})$  is the projection operator for right-(left-) handed quarks  $\hat{R}(\hat{L}) = (1 \pm \gamma_5)/2$ , and  $\hat{Q}_\pm$  is the projection operator  $\hat{Q}_\pm = (1 \pm \gamma_5 \mathcal{S}_\perp)/2$ , which projects out eigenstates of the transversely projected Pauli-Lubanski operator  $\mathcal{S}_\perp \gamma_5$  in a transversely projected nucleon.

The twist-four distributions are similar to those of twist-two, except they involve ‘bad’ components of the quark wavefunction

$$\begin{aligned} f_4(x) &= \frac{1}{\sqrt{2}} \sum_m \delta(p^+(1-x) - p_m^+) |\langle m | \psi_-(0) | P \rangle|^2, \\ g_3(x) &= \frac{1}{\sqrt{2}} \sum_m \delta(p^+(1-x) - p_m^+) [|\langle m | \hat{L} \psi_-(0) | PS_\parallel \rangle|^2 - |\langle m | \hat{R} \psi_-(0) | PS_\parallel \rangle|^2], \\ h_3(x) &= \frac{1}{\sqrt{2}} \sum_m \delta(p^+(1-x) - p_m^+) [|\langle m | \hat{Q}_+ \psi_-(0) | PS_\perp \rangle|^2 - |\langle m | \hat{Q}_- \psi_-(0) | PS_\perp \rangle|^2]. \end{aligned} \quad (19)$$

Here the distributions have been rescaled to make them dimensionless, and factors of  $(M/\Lambda)^2$  have been absorbed in the twist-four part of the density matrix,  $M(x)|_{\text{twist-4}}$ .

Note that the twist-two and twist-four distributions have a natural interpretation in the parton model, where they are related to the probability of finding a parton carrying fraction  $x$  of the plus component of momentum of the nucleon, and in the appropriate helicity or transversity eigenstates. In the twist-three case, the distributions do not have a similar interpretation in the parton model. However we can still guarantee momentum conservation by introducing a complete set of intermediate states,  $\sum_m |m\rangle \langle m|$ , and then write the distributions in terms of the matrix elements between nucleon states and



intermediate states

$$\begin{aligned}
e(x) &= \sum_m \delta(p^+(1-x) - p_m^+) \langle P | \psi^\dagger(0) | m \rangle_a (\gamma^0)_{ab} \langle m | \psi(0) | P \rangle_b, \\
h_L(x) &= \sum_m \delta(p^+(1-x) - p_m^+) \langle PS_{\parallel} | \psi^\dagger(0) | m \rangle_a (\gamma^3 \gamma^5)_{ab} \langle m | \psi(0) | PS_{\parallel} \rangle_b, \\
g_T(x) &= \sum_m \delta(p^+(1-x) - p_m^+) \langle PS_{\perp} | \psi^\dagger(0) | m \rangle_a (\gamma^0 \gamma^5 \not{x}_{\perp})_{ab} \langle m | \psi(0) | PS_{\perp} \rangle_b \quad (20)
\end{aligned}$$

where the matrix indices have been shown explicitly. Again the distributions have been rescaled so that they are dimensionless, absorbing factors of  $M/\Lambda$  into the density matrix  $M(x)|_{\text{twist-3}}$ .

The next step in the model calculation of the distributions is to form the momentum eigenstates  $|P\rangle$  and  $|m\rangle$  from the static states of the model. This can be done using either the Peierls-Yoccoz [19] projection, which gives a momentum dependent normalisation, or the Peierls-Thouless [20] projection, which leads to a more difficult calculation, but which preserves Galilean invariance of the matrix elements. Using either method, the correct support for the distributions is guaranteed by the above formalism. The distributions can then be calculated in terms of the Hill-Wheeler overlap integrals between the quark wavefunctions [13, 14].

Using the wavefunction of a model also introduces a scale  $\mu$  into the calculated distribution functions. This is the scale at which the model wavefunction is considered a good approximation to the true QCD wavefunction, which is presently unknown. The natural scale for the bag model, and most other phenomenological models employing light relativistic quarks, is the typical transverse momentum of the quarks,  $k_T \approx 400\text{MeV}$ . In order to compare a calculated distribution function with experiment, the calculated distribution needs to be evolved from the model scale up to the experimental scale  $Q^2$ . This has previ-

ously been done using leading order QCD evolution for the twist-2 distributions  $f_1(x)$  and  $g_1(x)$  [13, 14], with good agreement being obtained for a value of  $\mu$  in the region of 250 – 500 MeV. This could be criticised on the grounds that the strong coupling constant is not small in this region, however calculations using next to leading order evolution[21] also give good agreement with experiment for values of  $\mu \approx 350\text{MeV}$  and  $\alpha_S(Q^2 = \mu^2) \approx 0.75$ .

For the higher twist distributions there do not yet exist comprehensive calculations of the relevant anomalous dimensions for evolution of the distribution functions. For the twist-three distributions  $g_T$  and  $h_L$  full calculations of the anomalous dimensions have appeared in the literature [22, 23, 24]. For the lowest moments of these distributions ( $n = 3, 4$ ), the leading order evolution gives similar results to naive power counting for  $\sqrt{Q^2}$  in the region of 1 GeV. Thus we shall neglect QCD corrections to the evolution of the higher twist distributions, and use naive power counting to evolve these distributions.

In Figure 1 the nine twist-2, 3 and 4 distributions involving two quark correlation functions, calculated at the bag scale  $\mu$ , for a bag radius of 0.8 fm are shown. The Peierls-Yoccoz projection has been used to form the momentum eigenstates  $|p\rangle$  and  $|m\rangle$ , and only intermediate states containing two quarks have been considered. As is expected from equations (18, 19, 20), each of these distribution functions are similar in magnitude to one another. It is worth noting that the parton distributions satisfy the equalities

$$\begin{aligned}
f_1(x) + g_1(x) &= 2h_1(x) \\
e(x) + h_L(x) &= 2g_T(x) \\
f_4(x) + g_3(x) &= 2h_3(x)
\end{aligned} \tag{21}$$

which are the lower bounds of Soffer's inequalities[25].

The evolution of the twist-3 distributions is particularly interesting as the distributions have contributions from local operators of both twist-3 and twist-2. Hence the moments of the twist-3 distributions are related to the moments of the twist-2 distributions [7, 23, 24]

$$\begin{aligned}
\mathcal{M}_n[e] &= \frac{m}{M} \mathcal{M}_n[f_1] + \mathcal{M}_n[e^{(3)}] \\
\mathcal{M}_n[h_L] &= \frac{2}{n+2} \mathcal{M}_n[h_1] + \frac{n}{n+2} \frac{m}{M} \mathcal{M}_{n-1}[g_1] + \mathcal{M}_n[h_L^{(3)}] \\
\mathcal{M}_n[g_T] &= \frac{1}{n+1} \mathcal{M}_n[g_1] - \frac{1}{2} \frac{m}{M} \mathcal{M}_{n-1}[h_1] + \mathcal{M}_n[g_T^{(3)}]
\end{aligned} \tag{22}$$

where  $m$  is the quark mass,  $\mathcal{M}_n[f] = \int_0^1 x^n f(x) dx$  is the  $n$ th moment of the distribution  $f(x)$  and  $f^{(3)}$  denotes the genuine twist-3 part of the distribution  $f(x)$ . Note that when contributions from operators proportional to the quark mass or from twist-3 operators are ignored, the third of these relations is equivalent to the Wandzura-Wilczek relation [26]

$$g_2(x) = -g_1(x) + \int_x^1 \frac{g_1(y)}{y} dy. \tag{23}$$

In what follows we shall ignore terms directly proportional to the quark mass, as the masses of the  $u$  and  $d$  quarks are zero (or very small) in the MIT bag model. (If this discussion were extended to include strange quarks and anti-quarks then it would be important to keep terms in the quark mass.)

We can invert the moments above to find the genuine twist-3 parts of each distribution in terms of the calculated distributions and the twist-2 distributions

$$\begin{aligned}
e^{(3)}(x) &= e(x) \\
h_L^{(3)}(x) &= h_L(x) - 2x \int_x^1 \frac{dy}{y^2} h_1(y) \\
g_T^{(3)}(x) &= g_T(x) - \int_x^1 \frac{dy}{y} g_1(y).
\end{aligned} \tag{24}$$

This separation makes it possible to evolve the calculated distributions  $e, h_L, g_T$  from the model scale up to experimental scales. The procedure I use for the evolution is to separate the calculated distributions at the model scale  $Q^2 = \mu^2$  into twist-2 and twist-3 parts using eqn. (24). The twist-2 parts are then evolved using the Gribov-Lipatov-Altarelli-Parisi (GLAP) equation [27] to leading order, whereas the twist-3 parts are evolved according to naive power counting  $f^{(3)}(Q^2) \sim 1/\sqrt{Q^2}$ . The model scale has been chosen as  $\mu = 0.4$  GeV, and in Figure 2 the full twist-3 distributions at  $Q^2 = 1$  and 10 GeV<sup>2</sup> are shown. Comparing between  $e(x, Q^2)$ , which has no twist-2 part, and  $h_L(x, Q^2)$  and  $g_T(x, Q^2)$  enables us to see how the twist-2 parts of the latter two distributions dominate at higher  $Q^2$ .

In fact it is probably not a particularly good approximation to evolve  $e(x, Q^2)$  according to naive power counting. While a calculation of the anomalous dimensions for the operators contributing to  $e(x)$  has yet to be done, we can surmise a few facts about the lowest moments, including that the lowest moment of  $e(x)$  will have a small anomalous dimension despite the corresponding operator being twist-3. The relevant local operators for  $e(x)$  in the operator product expansion are

$$O^{\mu_1\mu_2\ldots\mu_n} = \mathcal{S}_n \bar{\psi}(iD^{\mu_1})(iD^{\mu_2})\ldots(iD^{\mu_n})\psi - \text{traces} \quad (25)$$

where  $\mathcal{S}_n$  symmetrizes over the Lorentz indices  $\mu_1, \ldots, \mu_n$ . The relevant matrix elements of these operators are

$$\langle P | O^{\mu_1\mu_2\ldots\mu_n} | P \rangle = 2M e_n P^{\mu_1} P^{\mu_2} \ldots P^{\mu_n} - \text{traces}. \quad (26)$$

Standard techniques give the sum rules

$$e_n = \int dx x^n e(x). \quad (27)$$

In particular, for  $n = 0$  we have

$$\int dx e(x) = \frac{1}{2M} \langle P | \bar{\psi} \psi | P \rangle \quad (28)$$

which is related to the nucleon  $\sigma$  term,  $\langle P | \frac{1}{2}(m_u + m_d)(\bar{u}u + \bar{d}d) | P \rangle$ . The  $\sigma$  term is renormalization point invariant in QCD, which implies that the matrix element in eqn. (28) will have an anomalous dimension of the same magnitude as that of the quark mass operator. Thus the zeroth moment of  $e(x)$  will change quite slowly with  $Q^2$ , whereas we expect that the higher moments should scale approximately as  $1/\sqrt{Q^2}$ . Thus the distribution  $e(x, Q^2)$  will tend to increase at low  $x$  and decrease at high  $x$  as  $Q^2$  increases<sup>2</sup>.

At twist-4 level there is no mixing of twist-2 and twist-3 operators with the local twist-4 operators [28], which simplifies the analysis somewhat. Of course there are a large number of local operators of twist-4 for each distribution function, and in the vast majority of cases their anomalous dimensions have not been calculated. Thus to evolve the twist-4 distributions  $f^4(x)$  naive power counting,  $f^4(x, Q^2) \sim 1/Q^2$  is again used. In Figure 3 we see the twist-4 distributions at  $Q^2 = 1$  and 10 GeV<sup>2</sup>, where again the bag scale has been taken as  $\mu = 0.4$  GeV.

Finally, the twist-two transversity distribution  $h_1(x)$  will be of interest at scales above 1 GeV<sup>2</sup>. The anomalous dimensions of the twist-2 operators have been calculated [29], so the evolution of the parton distribution from the bag scale is fairly straightforward. The results of this evolution up to  $Q^2 = 1$  GeV<sup>2</sup> and  $Q^2 = 10$  GeV<sup>2</sup> are shown in Figure 4.

---

<sup>2</sup>On completion of this work I learned of a calculation of the anomalous dimensions of  $e(x, Q^2)$  [41] which confirms these speculative remarks, in particular the anomalous dimensions of the operators corresponding to the second and third moments of  $e$  are similar in magnitude to the anomalous dimensions of twist-2 distributions.

## 4 Nucleon Structure Functions

The parton distribution functions calculated above can be measured in various processes, most notably deep inelastic lepton-nucleon scattering (DIS) and Drell-Yan (DY) processes. In this section we consider how the parton distributions combine to give the nucleon structure functions which can be measured in DIS, and those structure functions involving higher twist distributions which have been measured are compared with the calculated structure functions.

In the Bjorken limit ( $Q^2, \nu \rightarrow \infty$ ,  $x = Q^2/2(P \cdot q)$  fixed) the nucleon tensor  $W^{\mu\nu}$  can be expressed in terms of 14 structure functions [11]

$$\begin{aligned}
W^{\mu\nu} = & \left( -g^{\mu\nu} + \frac{q^\mu q^\nu}{q^2} \right) F_1(x) + \hat{p}^\mu \hat{p}^\nu \frac{F_2(x)}{\nu} \\
& + q^\mu q^\nu \frac{F_4(x)}{\nu} + (p^\mu q^\nu + p^\nu q^\mu) \frac{F_5(x)}{2\nu} \\
& - i\epsilon^{\mu\nu\alpha\beta} q_\alpha \left( p_\beta \frac{G_1(x)}{\nu} + M S_{\perp\beta} \frac{G_T(x)}{\nu} \right) \\
& + i\epsilon^{\mu\nu\alpha\beta} M p_\alpha S_{\perp\beta} \frac{G_3(x)}{\nu} + i\epsilon^{\mu\nu\alpha\beta} q_\alpha p_\beta \frac{F_3(x)}{2\nu} \\
& + \left( -g^{\mu\nu} + \frac{q^\mu q^\nu}{q^2} \right) a_1(x) + \hat{p}^\mu \hat{p}^\nu \frac{a_2(x)}{\nu} \\
& + q^\mu q^\nu \frac{a_4(x)}{\nu} + (p^\mu q^\nu + p^\nu q^\mu) \frac{a_5(x)}{2\nu} \\
& + M(S_{\perp}^\mu \hat{p}^\nu + S_{\perp}^\nu \hat{p}^\mu) \frac{b_1(x)}{2\nu} + M(S_{\perp}^\mu p^\nu + S_{\perp}^\nu p^\mu) \frac{b_2(x)}{2\nu}, \tag{29}
\end{aligned}$$

where the last seven structure functions ( $F_3, a_{1,2,4,5}, b_{1,2}$ ) are related to parity-violating processes involving the weak interaction. I have introduced the shorthand notation  $\hat{p}^\mu = p^\mu - \frac{p \cdot q}{q^2} q^\mu$ .

It is conventional to introduce longitudinal structure functions, describing the scatter-

ing when the exchanged vector boson is longitudinally polarised

$$\begin{aligned} F_L(x) &= F_2(x) \left( 1 + \frac{4M^2 x^2}{Q^2} \right) - 2xF_1(x) \\ a_L(x) &= a_2(x) \left( 1 + \frac{4M^2 x^2}{Q^2} \right) - 2xa_1(x). \end{aligned} \quad (30)$$

According to the Callen-Gross relation [30] both  $F_L$  and  $a_L$  vanish in the Bjorken limit, and, ignoring QCD radiative corrections and nucleon mass effects, both are twist-4 structure functions.

The fourteen structure functions can all be expressed in terms of parton distribution functions [11, 12, 28]. In the following all contributions from parton distributions with two or more light-cone fractions (ie distributions involving two quark fields plus one or two gluon fields and distributions involving four quark fields) will be dropped and the discussion is limited to the distributions calculated above. We also keep terms linear in the quark masses. The electroweak current  $J^\mu(\xi)$  of the quarks coupling to vector bosons is taken to be

$$J^\mu(\xi) = \bar{\psi}(\xi) \gamma^\mu (g_v + g_a \gamma_5) \psi(\xi) \quad (31)$$

where the vector and pseudo-vector couplings,  $g_v$  and  $g_a$  take the values of the standard model. Also, because weak currents can change quark flavour, the mass of a quark in the initial state is denoted as  $m_i$ , and the mass of a quark in the final state as  $m_f$ .

For unpolarised scattering there are five measureable structure functions.  $F_1$  and  $F_2$  (or  $F_L$ ) describe electromagnetic scattering,  $F_3$  is related to parity violating weak scattering, and  $F_4$  and  $F_5$  are related to the scattering of non-conserved currents. We have:

$$F_1(x) = \frac{1}{2} \sum_q (|g_{vq}|^2 + |g_{aq}|^2) f_1^q(x)$$

$$-\frac{M}{Q^2} \sum_q m_f (|g_{vq}|^2 - |g_{aq}|^2) x e^q(x) \quad (32)$$

$$F_L(x) = \frac{M^2}{Q^2} \sum_q (|g_{vq}|^2 + |g_{aq}|^2) 4x^3 f_4^q(x) - \frac{M}{Q^2} \sum_q [(m_i + m_f)|g_{vq}|^2 + (m_f - m_i)|g_{aq}|^2] 4x^2 e^q(x) \quad (33)$$

$$F_3(x) = \sum_q (-1)^q (|g_{vq}|^2 + |g_{aq}|^2) f_1^q(x) \quad (34)$$

where  $(-1)^q$  is +1 for quarks and -1 for antiquarks. Finally

$$F_4(x) = \frac{M}{Q^2} \sum_q [|g_{vq}|^2 (m_i - m_f) + |g_{aq}|^2 (m_i + m_f)] e^q(x) \quad (35)$$

$$F_5(x) = \frac{2Mx}{Q^2} \sum_q [|g_{vq}|^2 (m_i - m_f) + |g_{aq}|^2 (m_i + m_f)] e^q(x). \quad (36)$$

Thus  $F_L$ ,  $F_4$  and  $F_5$  are twist-four structure functions.

For scattering from a longitudinally polarised nucleon we have five structure functions:

$$G_1(x) = \frac{1}{2} \sum_q (|g_{vq}|^2 + |g_{aq}|^2) g_1^q(x) \quad (37)$$

$$a_1(x) = \frac{1}{2} \sum_q (-1)^q (|g_{vq}|^2 + |g_{aq}|^2) g_1^q(x) \quad (38)$$

$$a_L(x) = \frac{2Mx}{Q^2} \sum_q (-1)^q (|g_{vq}|^2 + |g_{aq}|^2) [-2Mx^2 g_3^q(x) + 2m_i x h_L^q(x)] \quad (39)$$

$$a_4(x) = \frac{M}{Q^2} \sum_q (-1)^q (|g_{vq}|^2 + |g_{aq}|^2) m_i x h_L^q(x) \quad (40)$$

$$a_5(x) = \frac{2Mx}{Q^2} \sum_q (-1)^q (|g_{vq}|^2 + |g_{aq}|^2) m_i x h_L^q(x). \quad (41)$$

The twist-2 distribution  $a_1$  is the longitudinally polarised analogue of  $F_3$ , and if it were measured the role of the axial anomaly in the interpretation of measurements of  $G_1$  would be much clearer[31]. The structure functions  $a_{L,4,5}$  are all twist-4, with  $a_{4,5}$  related to non-conserved currents.

For scattering from a transversely polarised nucleon there are four structure functions:

$$G_T(x) = \frac{1}{2} \sum_q (|g_{vq}|^2 + |g_{aq}|^2) g_T^q(x) \quad (42)$$



$$G_3(x) = \frac{1}{2M} \sum_q \left[ |g_{vq}|^2 (m_f - m_i) - |g_{aq}|^2 (m_i + m_f) \right] h_1^q(x) \quad (43)$$

$$b_1(x) = \sum_q (-1)^q (|g_{vq}|^2 + |g_{aq}|^2) x g_T^q(x) \quad (44)$$

$$b_2(x) = \frac{1}{M} \sum_q (-1)^q (|g_{vq}|^2 + |g_{aq}|^2) m_i h_1^q(x). \quad (45)$$

These four structure functions are twist-3.  $G_T = G_1 + G_2$  is related to the transverse spin of the quarks and antiquarks,  $b_1$  is its parity-violating partner, while  $G_3$  and  $b_2$  are related to non-conserved currents.

Many experiments over the years have determined  $F_1$ ,  $F_3$  and  $G_1$  to good precision, and in the near future  $G_T$  should be measured to similar precision.  $F_L$  has also been measured to a lower degree of precision, thus it should be possible for us to extract estimates of the parton distributions  $g_T$  and  $f_4$ . Unfortunately there is little hope of determining any of the other parton distributions from DIS. From the expressions for  $F_{4,5}$ , eqs. (35, 36) one might hope that  $e(x)$  would be measurable in heavy quark production. However because  $|g_{vq}| = |g_{aq}|$  the terms in  $m_f$  cancel<sup>3</sup>. A similar cancellation occurs in eqn. (43) making a determination of  $h_1(x)$  very difficult. However the possibility exists to measure  $h_{1,L}(x)$  and  $e(x)$  in polarised Drell-Yan processes [7] which may be possible at RHIC.

Previous calculations [13, 21] have shown good agreement between experimental data for  $F_1(x)$  and  $F_3(x)$  and the model predictions. We are now in a position to compare the model prediction for  $F_L(x)$  with experimental data. Experimentally the ratio  $R = F_L/2xF_1$  has been measured [3], and there is good evidence for a twist-4 contribution [32, 33] at medium and high  $x$  and  $Q^2 < 10 \text{ GeV}^2$ . Before we can compare with the data we should also take into account effects from perturbative QCD which give a non-zero

---

<sup>3</sup>This cancellation does not occur when the exchange boson is a Z boson, so there may exist a possibility to measure  $F_{4,5}$  at HERA

$F_L$  at leading and next-to-leading order, and effects from the target nucleon mass. In the simplest version of the bag model the twist four contribution to  $R$  for electromagnetic scattering is given by

$$R^{(4)}(x, Q^2) = \frac{8M^2 x^2}{Q^2} \frac{f_4(x, Q^2)}{f_1(x, Q^2)} \quad (46)$$

In Figure 5 we show our calculated  $R^{(4)}(x, Q^2)$  at  $Q^2 = 2$  and  $5 \text{ GeV}^2$ . We also show the experimental values of  $R$  and various perturbative QCD calculations, including target mass effects, and the effect of adding the twist-4 contribution from the bag model at these scales. Because  $R^{(4)}(x, Q^2)$  effectively scales as  $f_4(x, \mu^2)/Q^4$ , we calculate a large correction to the perturbative calculations at only low values of  $Q^2$ , however this twist-4 correction is in the right direction, and for low  $Q^2$  gives a good fit to the data at medium  $x$  values.

If the data at low  $Q^2$  improves in accuracy, it may be possible to perform an independent check on our value of the bag scale,  $\mu$ , from a fit of our calculated parton distribution  $f_4$  with the data at various values of  $Q^2$ .

The other higher twist structure function that has been measured is  $G_2(x) = G_T(x) - G_1(x)$  [6, 5]. In Figure 6 the experimental data for  $G_2^p(x)$  is compared with the calculated structure function at  $Q^2 = 5 \text{ GeV}^2$ . The calculation is in reasonable agreement with the data. In particular the calculated  $G_2(x)$  crosses the  $x$  axis in the right region. As this crossing is determined by the interplay between the twist-3 part of  $G_2(x)$ , given by  $g_T^{(3)}(x)$  and the twist-2 portion  $-g_1(x) + \int_x^1 dy g_1(y)/y$ , this gives us some confidence in our understanding of the relations between the twist-2 and twist-3 distributions. It will be interesting to check our model calculations against experimental at other values of  $Q^2$ . As

$Q^2$  increases we predict that the crossing point  $x_0$  where  $G_2(x_0) = 0$  will move to larger  $x$ .

It is also interesting to note that while the bag model calculation for the structure function  $G_1^p(x)$  is not particularly good, presumably because the calculation does not include effects arising from the axial anomaly[13], in the case of  $G_2^p(x)$  the agreement with the data is better, probably because of the cancellation between the two terms in the twist-2 part of  $G_2^p(x)$ .

Finally in Table 1 the calculated values for some of moments of the twist-2 and twist-3 parts of  $G_2^p(x)$  are displayed and compared with values from other calculations and those extracted from the experimental data.

Before concluding, there are some limitations to these calculations which should be borne in mind. There is no flavour dependence of the calculated parton distributions, so the distributions and structure functions shown above should be taken as applying to scattering from an isoscalar target. For our comparison of  $R$  this is not important, as experiment has shown no target dependence for  $R$  [3], but for  $G_2$  the flavour dependence will be as important as for  $G_1$ [13, 37]. In the model, the flavour dependence of the parton distributions comes from the  $SU(6)$  spin-flavour part of the wavefunction, and the one gluon exchange mechanism means that the two-quark intermediate state must be either a scalar ( $S=0$ ) or vector ( $S=1$ ) with masses  $m_s$  and  $m_v > m_s$ , respectively [34, 13]. Furthermore no account has been taken of contributions to the parton distributions from intermediate states consisting of four quarks. However these contributions have only a small effect on valence distributions, and this is all in the small  $x$  region [13], which is not of great importance here.

An important correction to the parton distributions will come from mesonic contributions via the so-called Sullivan process [35], where meson ( $\pi, \rho, K \dots$ ) exchange between the virtual photon and the nucleon occurs. These processes are known to lead to important modifications in the parton distributions at twist-2 [36, 37], particularly for  $g_1(x)$ , and there is no reason to suppose that the higher twist distributions should be unaffected. This should be important in the model calculation of the structure function  $G_2$ .

## 5 Summary

In this paper we have discussed the various parton distribution functions up to twist four in the context of the MIT bag model. The discussion has been limited to those distributions involving two-quark correlation functions, however these include effects from the bag boundary, which is a simple model of the effects of the gluon field. From the twist-3 distributions, which involve quark-gluon correlations, we have calculated the twist-3 structure function,  $G_2(x)$ , and found the calculation in good agreement with the experimental data, which gives us some confidence in using the bag as a model of the quark-gluon dynamics involved in DIS.

Four-quark correlation functions are expected to be small as they involve the calculation of Hill-Wheeler-type overlap functions for four quarks in the bag. Also these distributions are not directly accessible to experiment. However in future work we shall look at the corrections four-quark distributions make to the two-quark distributions calculated here.

At twist-four we have seen that the calculated distribution  $f_4(x)$  gives a contribution to the experimentally measured  $R = F_L/2xF_2$ . When added to the contributions from

perturbative QCD and target mass effects, the calculation gives good agreement with the data at  $Q^2 \sim 1 \text{ GeV}^2$  and medium values of  $x$ .

Some improvements can be made to our calculations. On the model side we can add flavour dependence to our distributions, and we can also add the important effects of the pion cloud. Also we can improve our evolution techniques for the distribution functions. For the twist-2 distributions next-to-leading-order QCD corrections are available. At twist-3 there have been recent developments in the calculations of anomalous dimensions of the relevant operators, so that a correct leading order QCD approach is possible, though this will be very difficult.

I would like to thank the Institute for Theoretical Physics, University of Adelaide, for hospitality and support while this work was in completion. I would also like to thank Tony Thomas, Fernando Steffens and Steve Shrimpton for valuable comments. This work was supported in part by the Australian Research Council.

## References

- [1] NMC, P. Amaudruz *et al.*, Phys. Rev. Lett. 66 (1991) 560; Phys. Lett. B 295 (1992) 159.
- [2] SMC, D. Adams *et al.*, Phys. Lett. B 329 (1994) 399.
- [3] E140X, S. Dasu *et al.*, Phys. Rev. D 49 (1994) 5641; L. H. Tao *et al.*, Z. Phys. C 70 (1996) 387.
- [4] E142, P. L. Anthony *et al.*, Phys. Rev. Lett. 71 (1993) 959.
- [5] SMC, D. Adams *et al.*, Phys. Lett. B 336 (1994) 125.
- [6] E143 K. Abe *et al.*, Phys. Rev. Lett. 76 (1996) 587.
- [7] R. L. Jaffe and X. Ji, Phys. Rev. Lett. 67 (1991) 552; R. L. Jaffe and X. Ji, Nucl. Phys. B 375 (1992) 527.
- [8] E. D. Bloom and F. J. Gilman, Phys. Rev. D 4 (1972) 2901.
- [9] X. Ji and P. Unrau, Phys. Rev. D 52 (1995) 72.
- [10] A. De Rújula, H. Georgi and H. D. Politzer, Ann. Phys. 103 (1977) 315.
- [11] X. Ji, Nucl. Phys. B 402 (1993) 217.
- [12] R. K. Ellis, W. Furmanski and R. Petronzio, Nucl. Phys. B 212 (1983) 29.
- [13] A. W. Schreiber, A. I. Signal and A. W. Thomas, Phys. Rev. D 44 (1991) 2653.
- [14] A. Ardekani and A. I. Signal, Phys. Lett. B 311 (1993) 281.

- [15] J. Kogut and D. E. Soper, Phys. Rev. D 1 (1970) 2901.
- [16] A. Chodos, R. L. Jaffe, K. Johnson, C. B. Thorn and V. F. Weisskopf, Phys. Rev. D 9 (1974) 3471.
- [17] M. R. Bate and A. I. Signal, J. Phys. G 18 (1992) 1875; E. Naar and M. C. Birse, Phys. Lett. B 305 (1993) 190.
- [18] A. I. Signal and A. W. Thomas, Phys. Rev. D 40 (1989) 2832.
- [19] R. E. Peierls and J. Yoccoz, Proc. Phys. Soc. A 70 (1957) 381.
- [20] R. E. Peierls and D. J. Thouless, Nucl. Phys. 38 (1962) 154.
- [21] F. M. Steffens and A. W. Thomas, Adelaide preprint ADP-94-27/T166 (1994).
- [22] E. V. Shuryak and A. I. Vainshtein, Nucl. Phys. B 201 (1982) 141.
- [23] J. Kodaira, Y. Yasui and T. Uematsu, Phys. Lett. B 344 (1995) 348.
- [24] Y. Koike and K. Tanaka, Phys. Rev. D 51 (1995) 6125.
- [25] J. Soffer, Phys. Rev. Lett. 74 (1995) 1292.
- [26] S. Wandzura and F. Wilczek, Phys. Lett. B 72 (1977) 195.
- [27] V. N. Gribov and L. N. Lipatov, Sov. J. Nucl. Phys. 15 (1972) 438; L. N. Lipatov, *ibid.* 20 (1975) 94; G. Altarelli and G. Parisi, Nucl. Phys. B 126 (1977) 298.
- [28] R. L. Jaffe and M. Soldate, Phys. Rev. D 26 (1982) 49.
- [29] X. Artru and M. Mekhfi, Z. Phys. C 45 (1990) 669.

- [30] C. G. Callen and D. G. Gross, Phys. Rev. Lett. 22 (1969) 156.
- [31] S. D. Bass and A. W. Thomas, Prog. Part. Nucl. Phys. 33 (1994) 449.
- [32] J. L. Miramontes, M. A. Miramontes and J. Sanchez Guillén, Phys. Rev. D 40 (1989) 2184; J. Sanchez Guillén *et al.*, Nucl. Phys. B 353 (1991) 337.
- [33] A. Bodek, S. Rock and U. K. Yang, Rochester preprint UR-1355, to be published in Z. Phys. C.
- [34] F. E. Close and A. W. Thomas, Phys. Lett. B 212 (1988) 227.
- [35] J. D. Sullivan, Phys. Rev. D 5 (1972) 1732.
- [36] A. W. Schreiber, P. J. Mulders, A. I. Signal and A. W. Thomas, Phys. Rev. D 45 (1992) 3069.
- [37] F. M. Steffens, H. Holtmann and A. W. Thomas, Phys. Lett. B 358 (1995) 139.
- [38] X. Song, Phys. Rev. D 54 (1996) 1955.
- [39] M. Gockler *et al.*, Phys. Rev. D 53 (1996) 2317.
- [40] E. Stein *et al.*, Phys. Lett. B 343 (1995) 369.
- [41] Y. Koike and N. Nishiyama, preprint hep-ph/9609207.



## Figure Captions

**Figure 1.** The parton distribution functions calculated at the bag scale  $Q^2 = \mu^2$ .

(a) The twist-two distributions  $f_1(x)$ ,  $g_1(x)$  and  $h_1(x)$ . (b) The twist-three distributions  $e(x)$ ,  $h_L(x)$  and  $g_T(x)$ . (c) The twist-four distributions  $f_4(x)$ ,  $g_3(x)$  and  $h_3(x)$ .

**Figure 2.** The twist-three parton distributions at (a)  $Q^2 = 1 \text{ GeV}^2$  and (b)  $Q^2 = 10 \text{ GeV}^2$ .

**Figure 3.** The twist-four parton distributions at (a)  $Q^2 = 1 \text{ GeV}^2$  and (b)  $Q^2 = 10 \text{ GeV}^2$ .

**Figure 4.** The transversity dependent twist-two parton distribution  $h_1(x, Q^2)$  at  $Q^2 = 1 \text{ GeV}^2$  and  $Q^2 = 10 \text{ GeV}^2$ .

**Figure 5(a).** The twist-four distribution  $R^{(4)}(x, Q^2)$  calculated at  $Q^2 = 2 \text{ GeV}^2$  and  $Q^2 = 5 \text{ GeV}^2$ .

**Figure 5(b).** Experimental data [3] on  $R$  and QCD calculations with (upper band) and without (lower band) the twist-four contribution  $R^{(4)}(x)$  at  $Q^2 = 2 \text{ GeV}^2$ .

**Figure 6.** Comparison of experimental data [6] on  $G_2^p(x)$  with this calculation.

	$\mathcal{M}_2[G_2^p]$	$\mathcal{M}_4[G_2^p]$	$\mathcal{M}_6[G_2^p]$
This work	$-5.9 \times 10^{-3}$	$-1.2 \times 10^{-3}$	$-0.3 \times 10^{-3}$
C.M. Bag Model[38]	$-1.2 \times 10^{-3}$		
Lattice QCD[39]	$(-26.1 \pm 3.8) \times 10^{-3}$		
Data[6]	$(-6.3 \pm 1.8) \times 10^{-3}$	$(-2.3 \pm 0.6) \times 10^{-3}$	$(-1.0 \pm 0.3) \times 10^{-3}$

	$d_2^p$	$d_4^p$	$d_6^p$
This work	$6.3 \times 10^{-3}$	$1.3 \times 10^{-3}$	$0.3 \times 10^{-3}$
C.M. Bag Model	$-17.4 \times 10^{-3}$		
Lattice QCD	$(-48 \pm 5) \times 10^{-3}$		
QCD Sum Rule[40]	$(-6 \pm 3) \times 10^{-3}$		
Data[6]	$(5.4 \pm 5) \times 10^{-3}$	$(0.7 \pm 1.7) \times 10^{-3}$	$(0.1 \pm 0.8) \times 10^{-3}$

**Table 1.** Comparison of various calculations with experimental data for the moments of

$G_2^p$  and the twist-3 matrix elements  $d_n^p = 2(\frac{n+1}{n}\mathcal{M}_n[G_2^p] + \mathcal{M}_n[G_1^p]) = 2\frac{n+1}{n}\mathcal{M}_n[G_T^{(3)p}]$ .

Fig. 1(a) Twist-2 Parton Distributions

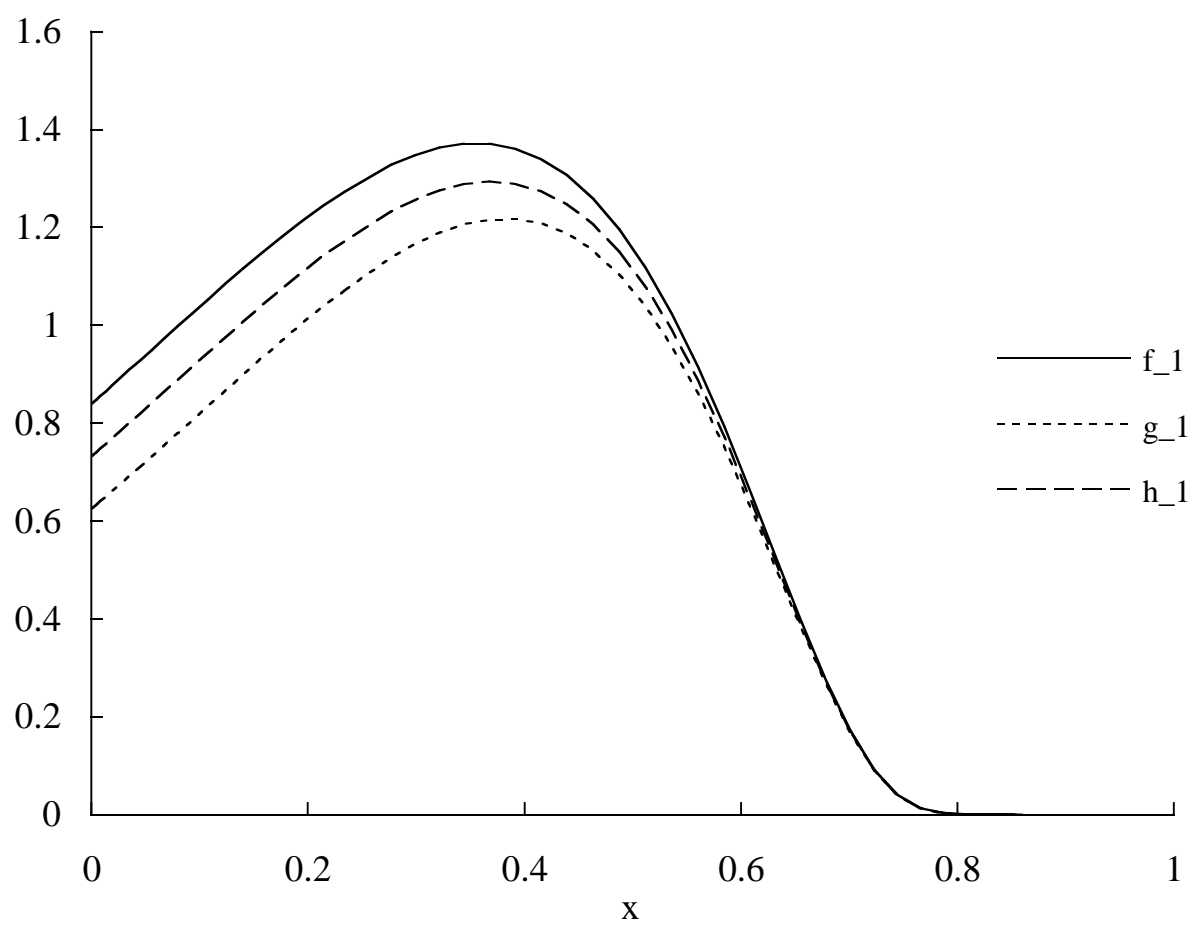


Fig. 1(b) Twist-3 Parton Distributions

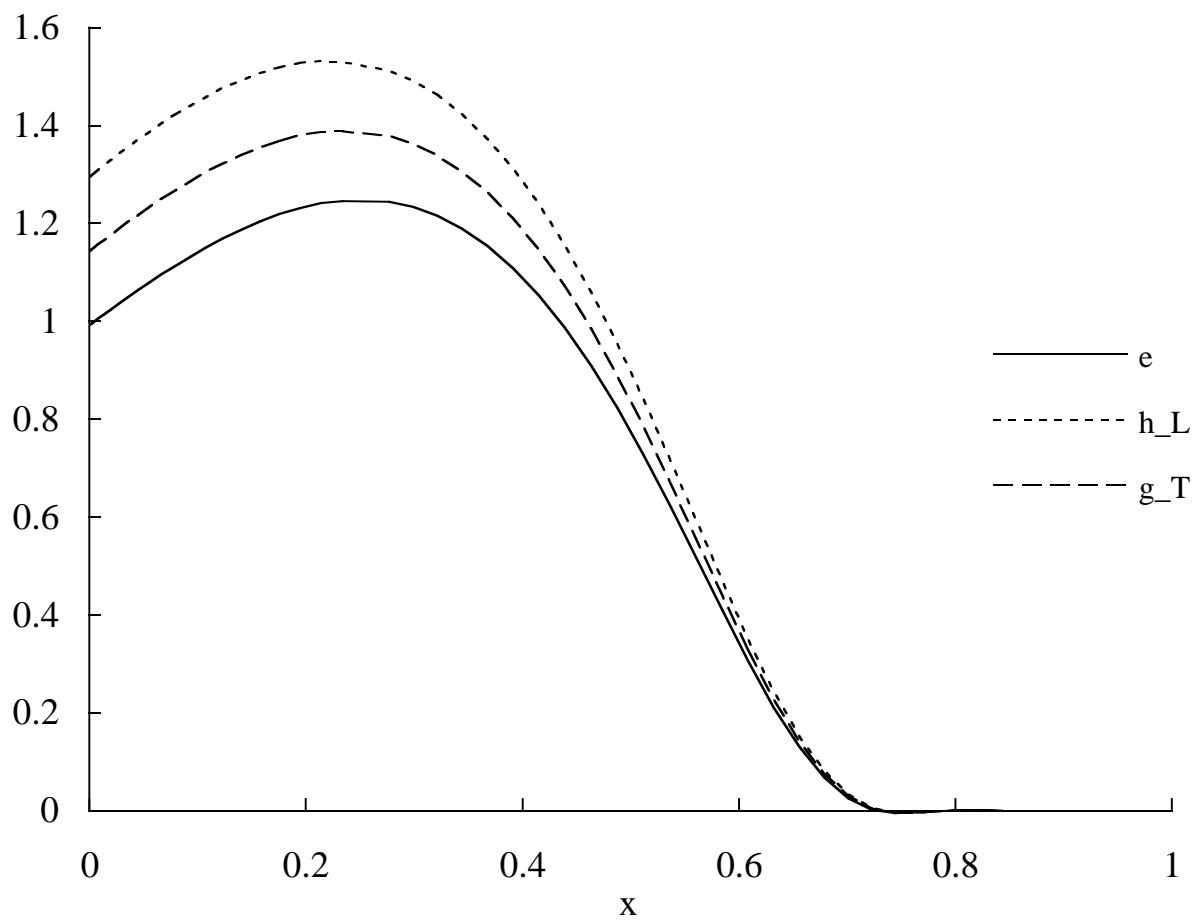


Fig. 1(c) Twist-4 Parton Distributions

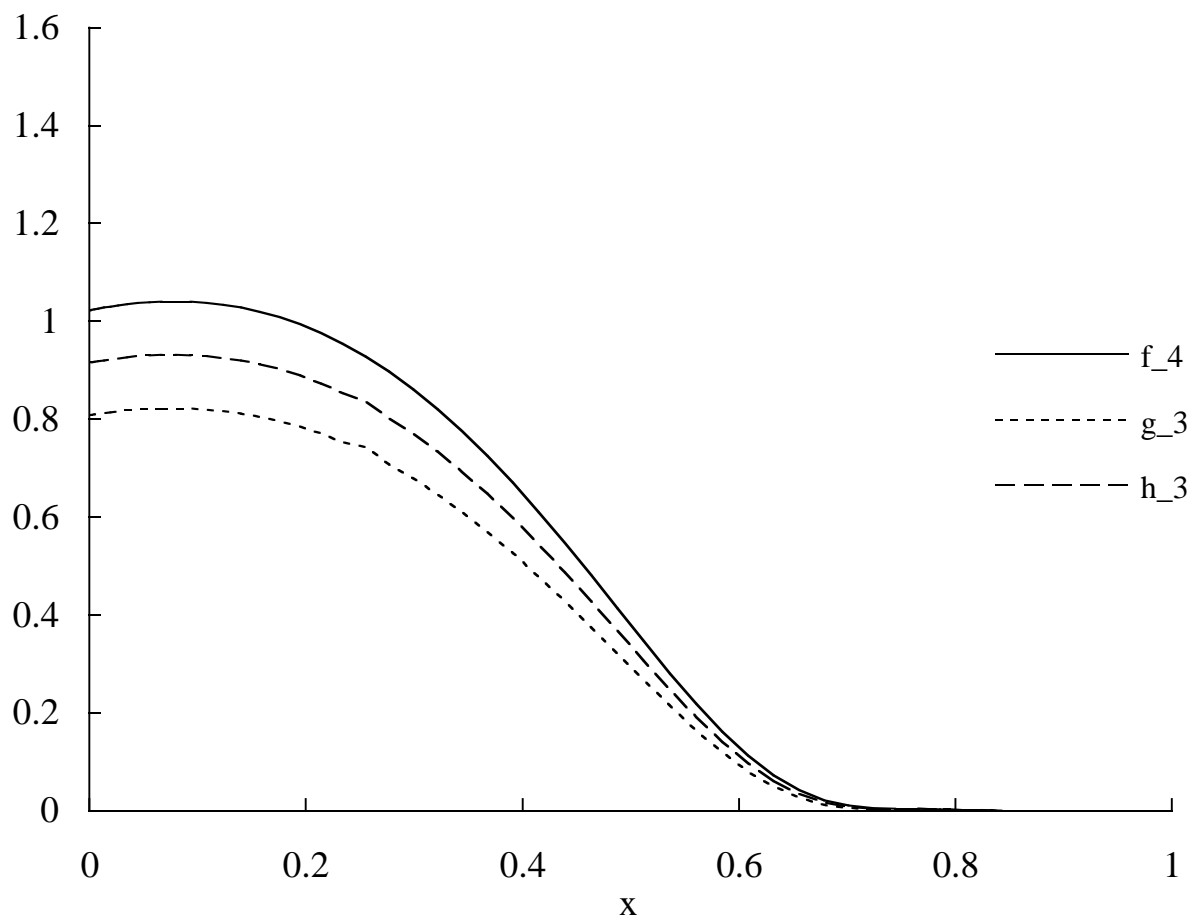


Fig. 2(a) Twist-3 Parton Distributions

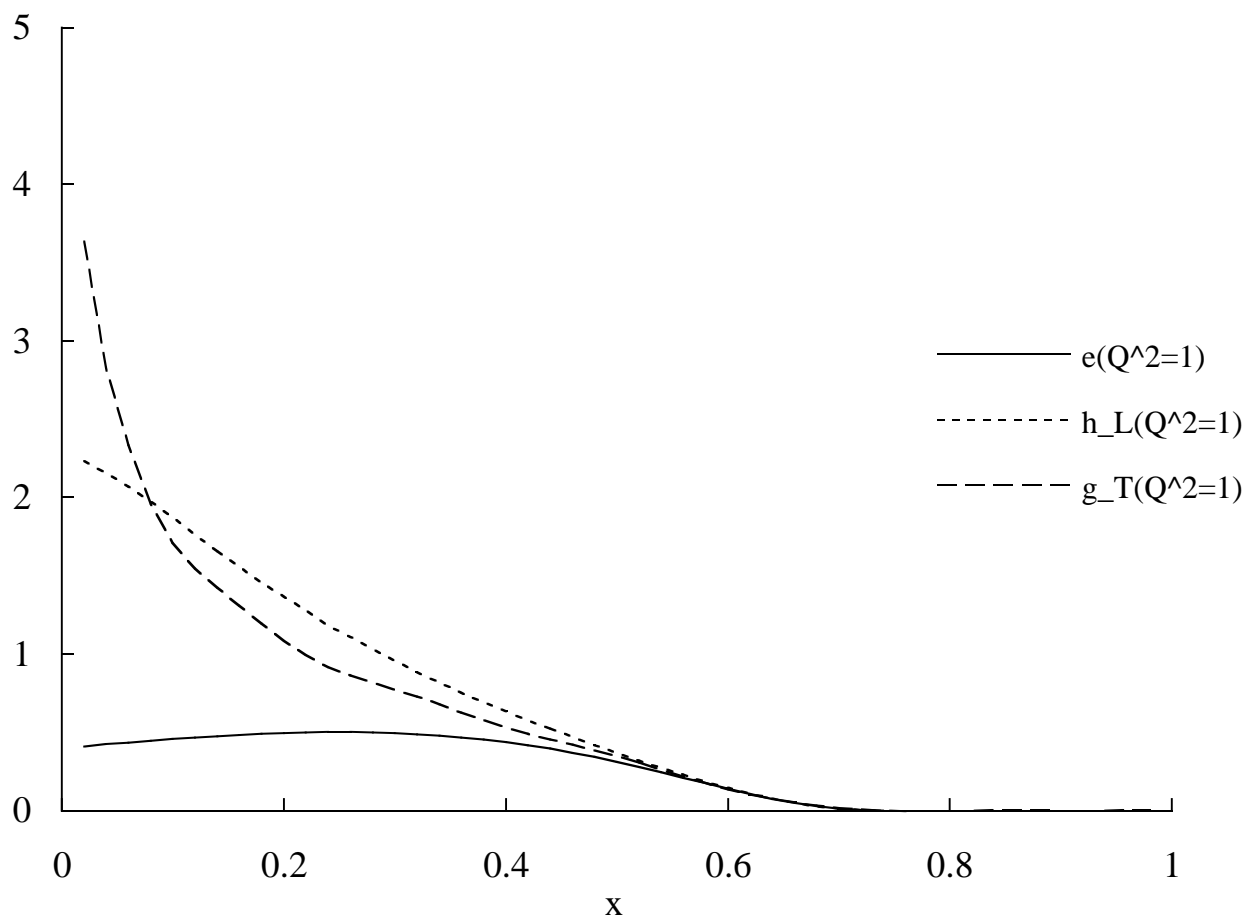


Fig. 2(b) Twist-3 Parton Distributions

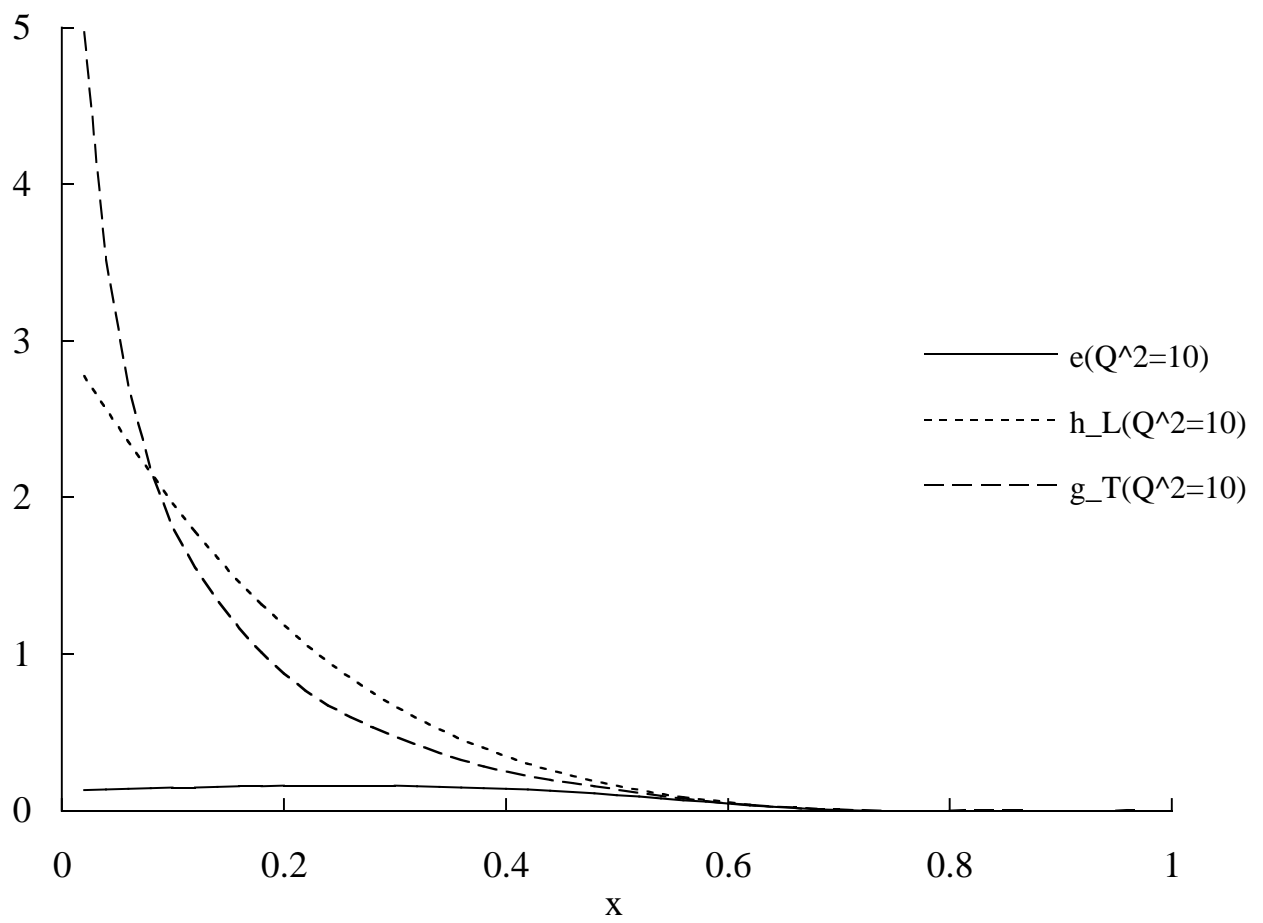


Fig. 3(a) Twist-4 Parton Distributions

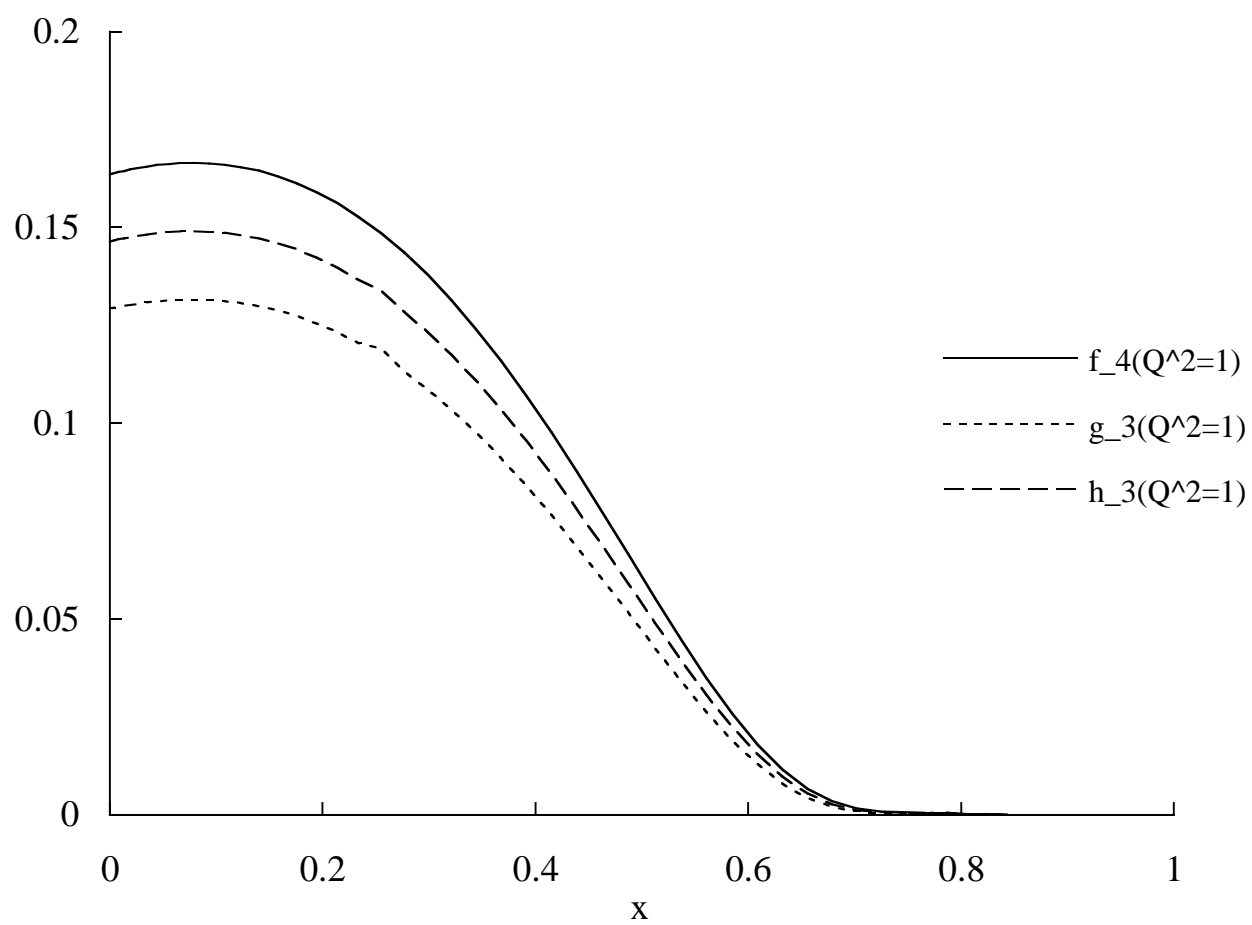




Fig. 3(b) Twist-4 Parton Distributions

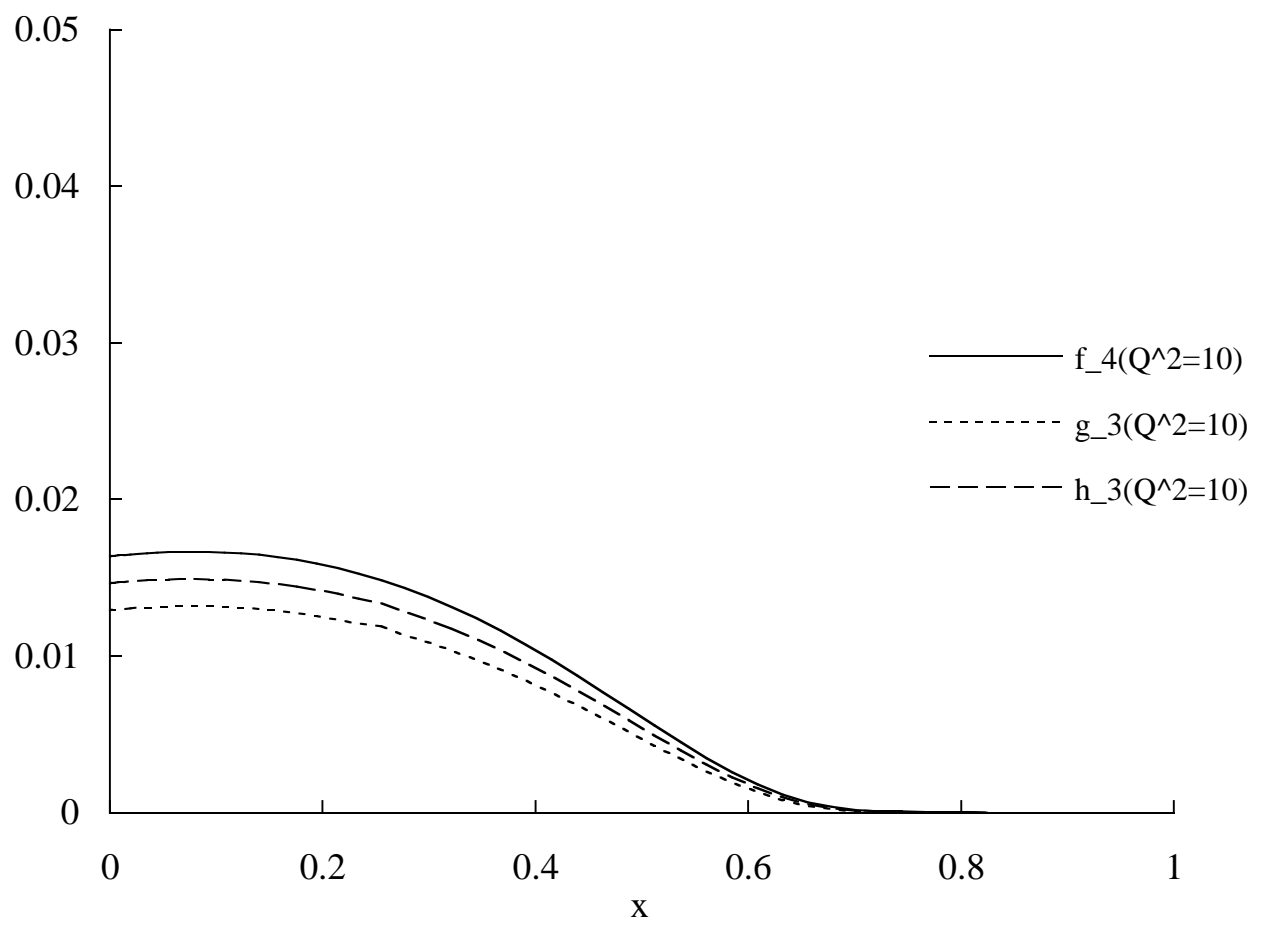


Fig. 4 Twist-2 Transversity Distribution

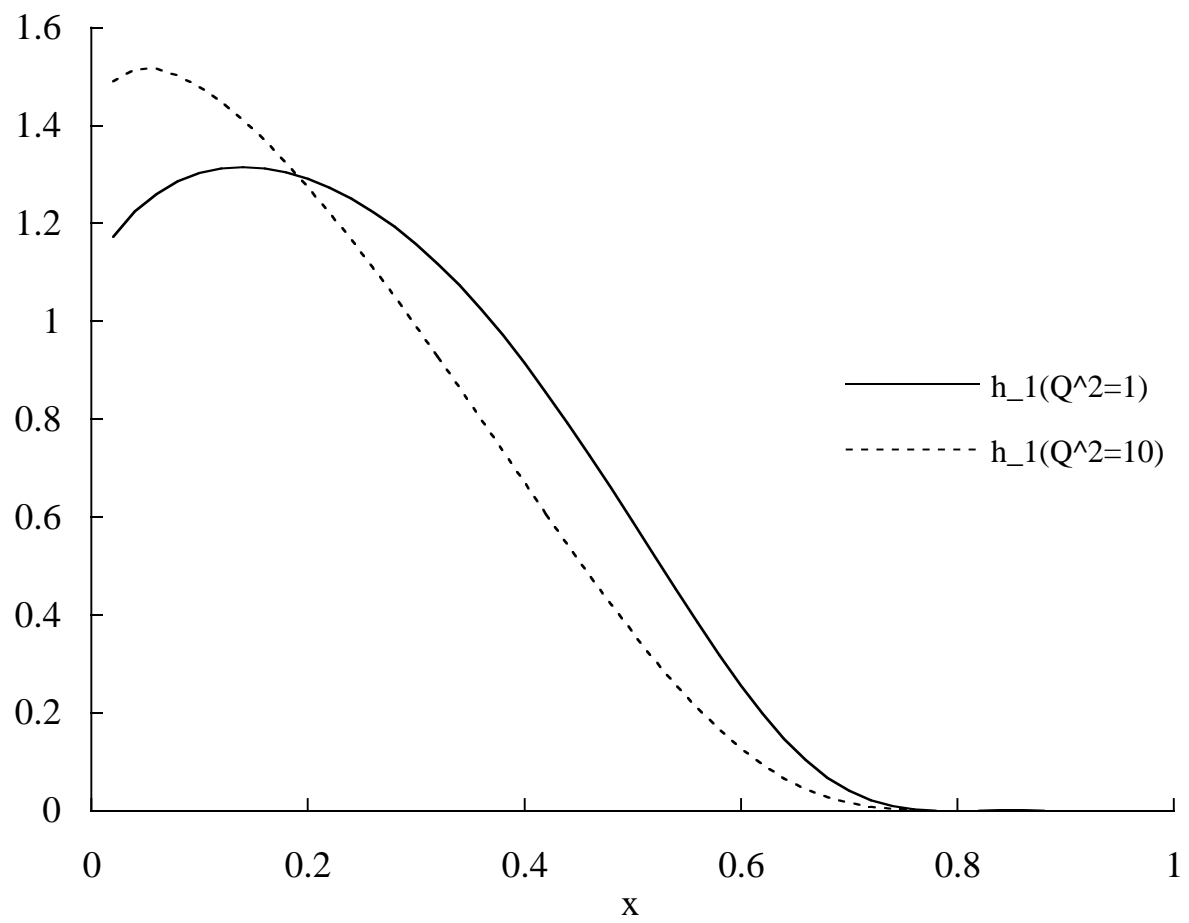


Fig. 5(a) Twist-4 Contribution to  $R$

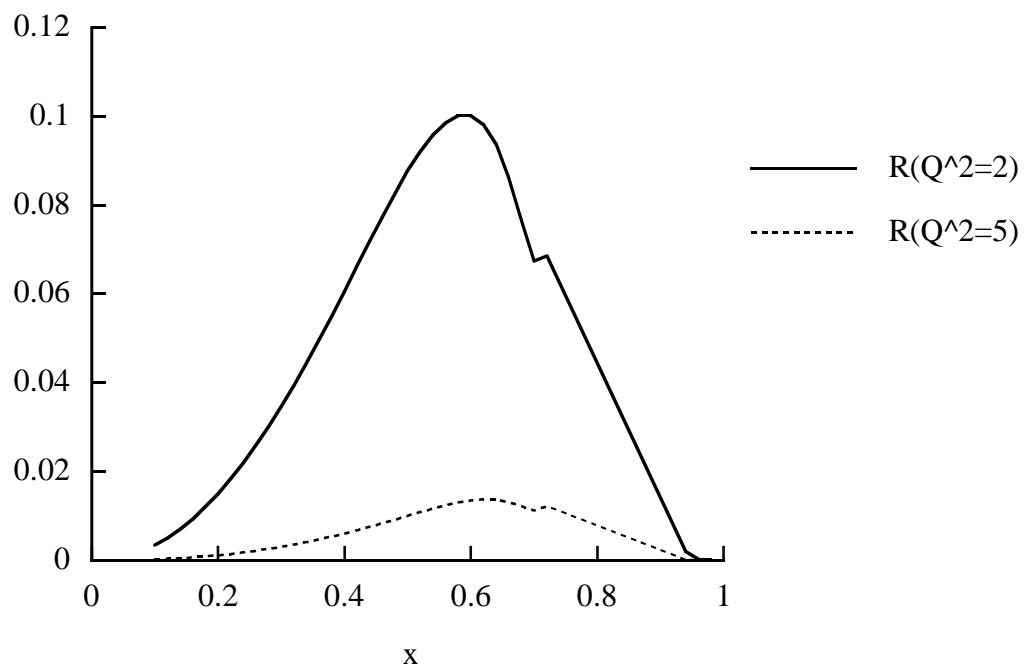


Fig. 5(b)  $R(x, Q^2 = 2 \text{ GeV}^2)$

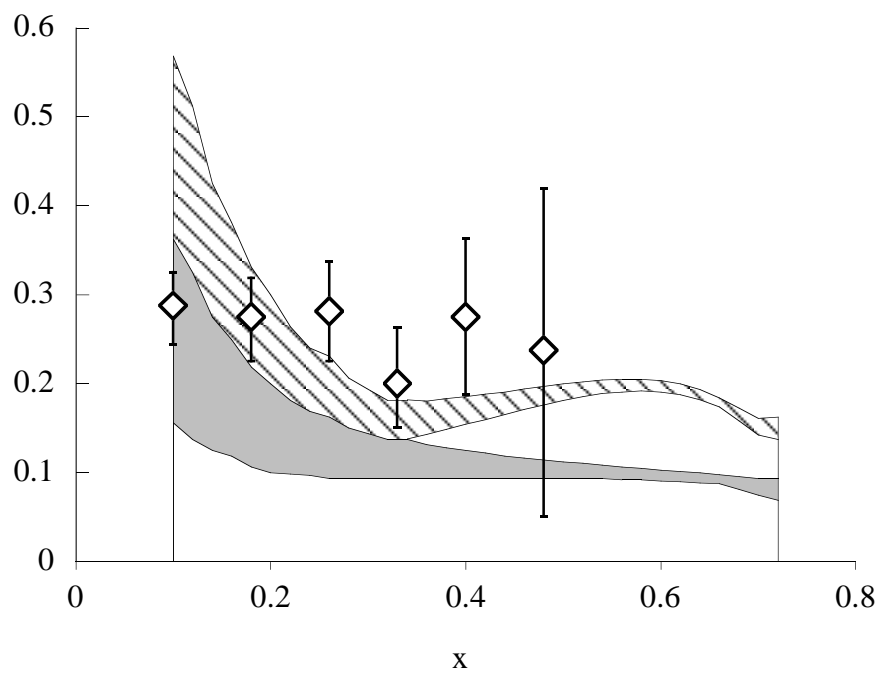


Fig. 6  $xG_2^p(x)$

